Vapor liquid solid-hydride vapor phase epitaxy (VLS-HVPE) growth of ultra-long defect-free GaAs nanowires: Ab initio simulations supporting center nucleation

Yamina Andre, Kaddour Lekhal, Philip Hoggan, Geoffrey Avit, Fabian Cadiz, Alistair Rowe, Daniel Paget, Elodie Petit, Christine Leroux, Agnes Trassoudaine, et al.

Vapor liquid solid-hydride vapor phase epitaxy (VLS-HVPE) growth of ultra-long defect-free GaAs nanowires: Ab initio simulations supporting center nucleation

Yamina André' , Kaddour Lekhal, Philip Hoggan, Geoffrey Avit, Fabian Cadiz, Alistair Rowe, Daniel Paget, Elodie Petit, Christine Leroux, Agnès Trassoudaine, M. Réda Ramdani, Guillaume Monier, David Colas, Rabih Ajib, Dominique Castelluci, and Evelyne Gil

Citation: The Journal of Chemical Physics **140**, 194706 (2014); doi: 10.1063/1.4874875
View online: http://dx.doi.org/10.1063/1.4874875
View Table of Contents: http://aip.scitation.org/toc/jcp/140/19
Published by the American Institute of Physics

Vapor liquid solid-hydride vapor phase epitaxy (VLS-HVPE) growth of ultra-long defect-free GaAs nanowires: *Ab initio* simulations supporting center nucleation

Yamina André,[1,2,a)] Kaddour Lekhal,[1,2] Philip Hoggan,[1,2] Geoffrey Avit,[1,2] Fabian Cadiz,[3] Alistair Rowe,[3] Daniel Paget,[3] Elodie Petit,[4,5] Christine Leroux,[6,7] Agnès Trassoudaine,[1,2,8] M. Réda Ramdani,[1,2] Guillaume Monier,[1,2] David Colas,[1,2] Rabih Ajib,[1,2] Dominique Castelluci,[1,2] and Evelyne Gil[1,2]

[1]*Clermont Université, Université Blaise Pascal, Institut Pascal, BP 10448, F-63000 Clermont-Ferrand, France*
[2]*CNRS, UMR6602, Institut Pascal, F-63171 Aubière, France*
[3]*Physique de la matière condensée, Ecole Polytechnique CNRS, Palaiseau, France*
[4]*Clermont Université, Université Blaise Pascal, Institut de Chimie de Clermont-Ferrand, BP 10448, F-63000 Clermont-Ferrand, France*
[5]*CNRS, UMR 6296, ICCF, F-63171 Aubière, France*
[6]*Université de Toulon, IM2NP, Bât. R, B.P. 20132, 83957 La Garde Cedex, France*
[7]*CNRS, UMR 7334, 83957 La Garde Cedex*
[8]*Clermont Université, Université d'Auvergne, BP 10448, F-63000 Clermont-Ferrand, France*

(Received 17 February 2014; accepted 16 April 2014; published online 21 May 2014)

High aspect ratio, rod-like and single crystal phase GaAs nanowires (NWs) were grown by gold catalyst-assisted hydride vapor phase epitaxy (HVPE). High resolution transmission electron microscopy and micro-Raman spectroscopy revealed polytypism-free zinc blende (ZB) NWs over lengths of several tens of micrometers for a mean diameter of 50 nm. Micro-photoluminescence studies of individual NWs showed linewidths smaller than those reported elsewhere which is consistent with the crystalline quality of the NWs. HVPE makes use of chloride growth precursors GaCl of which high decomposition frequency after adsorption onto the liquid droplet catalysts, favors a direct and rapid introduction of the Ga atoms from the vapor phase into the droplets. High influxes of Ga and As species then yield high axial growth rate of more than 100 μm/h. The diffusion of the Ga atoms in the liquid droplet towards the interface between the liquid and the solid nanowire was investigated by using density functional theory calculations. The diffusion coefficient of Ga atoms was estimated to be 3×10^{-9} m^2/s. The fast diffusion of Ga in the droplet favors nucleation at the liquid-solid line interface at the center of the NW. This is further evidence, provided by an alternative epitaxial method with respect to metal-organic vapor phase epitaxy and molecular beam epitaxy, of the current assumption which states that this type of nucleation should always lead to the formation of the ZB cubic phase. © *2014 AIP Publishing LLC*. [http://dx.doi.org/10.1063/1.4874875]

I. INTRODUCTION

The growth of nanostructures has been rapidly developing over the past decade. Among those structures, nanowires (NWs) have attracted much attention due to their surface/volume ratio morphology which yields particular properties, making them suitable for new nanoscale electronics,[1] photonics[2] and photo-voltaic[3,4] applications.

Catalyst-assisted and catalyst-free GaAs NWs grown by epitaxial techniques[5–8] may exhibit twins or stacking faults (SFs). GaAs NWs were shown to adopt the wurtzite (WZ) structure when the diameter is below 40 nm,[9] in contrast to the stable zinc blende (ZB) phase found in the bulk form of GaAs. The difference between ZB and WZ crystals lies in the stacking of the bilayers composing the crystal. ZB lattices follow an ABCABC stacking sequence and WZ lattices follow an ABABAB stacking sequence, where each letter represents a bilayer of III–V pairs.[10] A simple rotation of the stacking sequence on the growth direction ⟨111⟩ leads to the formation of the ZB or WZ phase. It has been shown that SFs are detrimental to both optical and electrical properties of NWs.[11–13] Therefore the control of the phase purity is one of the major challenges in NW technology. Several theoretical models have been developed in order to predict the crystalline structure adopted by GaAs NWs and clarify the origin of the formation of the SFs in NWs. When a vapor-liquid-solid (VLS) interface is involved, i.e., for catalyst-assisted growth being self-catalyzed or foreign metal-assisted growth, the nucleation step and the surface energies are suggested as responsible for the instability of the ZB phase in GaAs NWs. The WZ phase is formed when the nucleation step occurs at the edge of the catalyst particle-NW interface, that is at the triple phase vapor-liquid-solid line.[14] The contribution of the surface energies is major due to the high surface-to-volume ratio of NWs.[14] The growth parameters, such as the substrate temperature and the V/III flux ratio, also strongly influence the crystal phase of III-V NWs[8,14,15] by varying the liquid supersaturation in the catalyst droplet.

[a)]Author to whom correspondence should be addressed. Electronic mail: yamina.andre@univ-bpclermont.fr

Great effort has been devoted to improve the quality of GaAs NWs. Krogstrup *et al.*[16] demonstrated the growth of ZB GaAs NWs by Ga catalyst-assisted molecular beam epitaxy (MBE), with diameter down to 20 nm and length lower than 10 μm, exhibiting few twin planes at the bottom. Shtrikman *et al.*[17] achieved the growth of pure ZB tapered GaAs NWs by locally reducing the supersaturation of the Au-Ga catalyst droplet. Twin free ZB GaAs NWs with diameter between 30 and 50 nm on typical length of some micrometers were grown by metal-organic vapor phase epitaxy (MOVPE) implementing controlled experimental parameters of temperature and V/III ratio, which should be low and high, respectively.[18–20]

In this paper, we present the Au catalyst-assisted growth of GaAs nanowires by using the hydride vapor phase epitaxy (HVPE) process. HVPE makes use of GaCl growth precursors. It is interesting to investigate such a process since the physics of growth related to chloride precursors is different from the physics associated with metal-organic precursors. We have already demonstrated the feasibility of NWs growth by catalyst-assisted HVPE.[21,22] GaAs NWs synthesized by HVPE are grown at high axial growth rate (higher than 100 μm/h). They exhibit constant diameter on length varying from some micrometers to several tens of micrometers and were shown to be pure zinc blende for a mean diameter of 120 nm.[21] We focus here on the crystal and optical characterizations of GaAs NWs grown by HVPE with a 50 nm mean diameter. Related theoretical investigations based upon DFT Car-Parrinello dynamics simulations of the mechanism governing the Ga diffusion in the catalyst droplet are discussed in order to analyze the exceptional high HVPE growth rate and the stability of the structure of NWs grown by HVPE over length of several tens of microns.

II. VLS-HVPE GROWTH PROCESS

The growth of GaAs by HVPE involves gaseous GaCl molecules synthesized inside a horizontal hot wall quartz reactor by the use of HCl flow reacting with a Ga liquid source. Element V is transported as arsine (AsH_3) which is completely decomposed into ($As_2 \Leftrightarrow As_4$, considered at equilibrium) molecules when entering the hot wall reactor[23] The global growth reaction for GaAs in H_2 atmosphere is

$$GaCl_g + \frac{1}{4}As_{4g} + H_{2g} \rightleftharpoons GaAs + HCl_g + \frac{1}{2}H_{2g}.$$

The use of chloride molecules as element III growth precursors gives to HVPE its main feature: the dechlorination frequency is high enough to avoid kinetic limitation and conditions for equilibrium are quickly reached.[24–26] A wide range of growth rates (from 3 to 100 μm/h) can then be obtained by immediate influence of an increase (or a decrease) of the vapor phase supersaturation. The latter (γ) is defined as the actual partial pressures ratio above the substrate, to the equilibrium partial pressures ratio of the growth reaction which is given by $K(T)$, the reaction equilibrium constant at temperature T:

$$\gamma = \frac{[GaCl][As_4]^{1/4}[H_2]^{1/2}}{[HCl]K(T)} - 1$$
$$K(T) = \frac{[GaCl]_{eq}[As_4]_{eq}^{1/4}[H_2]_{eq}^{1/2}}{[HCl]_{eq}},$$

where [i] is the partial pressure of gaseous species i above the substrate. $K(T)$ is determined by calculating the variation of the Gibbs energy related to the growth reaction. The supersaturation can be tuned by varying the temperature and the partial pressures of GaCl, As_4, and additional HCl in the vapor phase.[26]

Prior to HVPE growth, a sub-monolayer of gold was deposited on 4° misoriented vicinal (001) GaAs substrates in an ultra-high vacuum (UHV) evaporator system (at 10^{-6} Pa). The thickness of the Au layer, 1 Å, was controlled by using x-ray photoelectron spectroscopy (XPS) calibration.[27,28] Au-covered substrates were introduced into the HVPE reactor to be heated from room temperature to the growth temperature, namely 715 °C. During this step, the substrates were kept in an under-saturated As_2/As_4 atmosphere to favor the formation of Au-Ga liquid droplets on the surface.[29] The GaAs growth was carried out under a H_2 vector flow of 3000 cm^3/min, with a III/V ratio (ratio of the GaCl partial pressure to the As_4 partial pressure above the substrate) of 4.4, which are standard experimental conditions for the growth of GaAs by HVPE.[26]

Dense arrays of uniform and ultra-long GaAs NWs were obtained for a growth time of 30 min (Fig. 1(a)) on (001) GaAs substrates covered by an Au film annealed in the HVPE reactor before NW growth. The NWs exhibit lengths as long as 100 μm with a mean diameter of 50 nm. Upon heating prior to growth, one expects de-cohesion of the Au film, random Au diffusion, and self-assembly into Au particles of various diameters on the substrate surface,[30,31] as shown on the

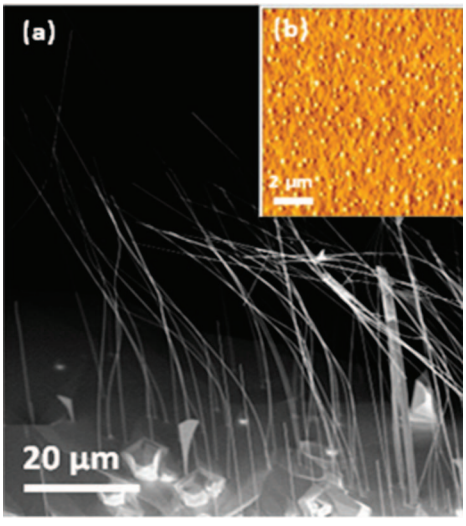

FIG. 1. (a) Top view SEM image of the (001) GaAs substrate edge showing GaAs nanowires a few tens of micrometers long, oriented along the (111)B direction, grown by Au-assisted VLS-HVPE at 715 °C during 30 min. The NWs were bent when exposed to the electron beam. (b) As an insert, AFM image of the surface of the Au-covered GaAs (001) substrate after annealing between room temperature and growth temperature (715 °C) in the HVPE reactor.

AFM image recorded after the annealing step of the Au/GaAs substrate (Fig. 1(b)). This pre-growth annealing carried out at 715 °C under an intentional dearth of As, results in a rough Au-Ga surface layer with a significant liquid Ga coverage.

For microluminescence investigations, the nanowires were isolated from the substrate after mechanical separation and deposited on a silicon substrate. The silicon substrate was patterned with an alumina labeled grid in order to allow a precise localization of an individual nanowire using optical and electron microscopy (Fig. 2(a)). Microluminescence investigations were performed as a function of temperature down to 6 K using an experiment described elsewhere.[32] The experimental setup consists of a modified commercial microscope which allows us to locally focus the laser excitation (Gaussian radius 0.6 μm, power 1 mW) and to take the image of the light emission with a CCD camera. It was also possible to take a spectrum of the emission in an adjustable point of the image, using a multi-mode optical fiber at the output of which the spectrum is analyzed by a spectrometer and a CCD camera. Shown in Fig. 2(b) is a microluminescence image taken for a laser spot focused near the middle of the NW.

Several groups have performed PL measurements on NWs grown by Au-catalyst assisted MBE and MOVPE exhibiting ZB-WZ polytypism to demonstrate the ZB structure as a function of the experimental growth parameters. For low temperature measurements in the range of [5–15] K, the WZ structure is reported as a broad peak at 1.478 eV attributed to the direct exciton transition;[33] the ZB exciton luminescence is respectively reported as an intense peak at 1.519 eV,[33] 1.515 eV,[18] and 1.529 eV.[34]

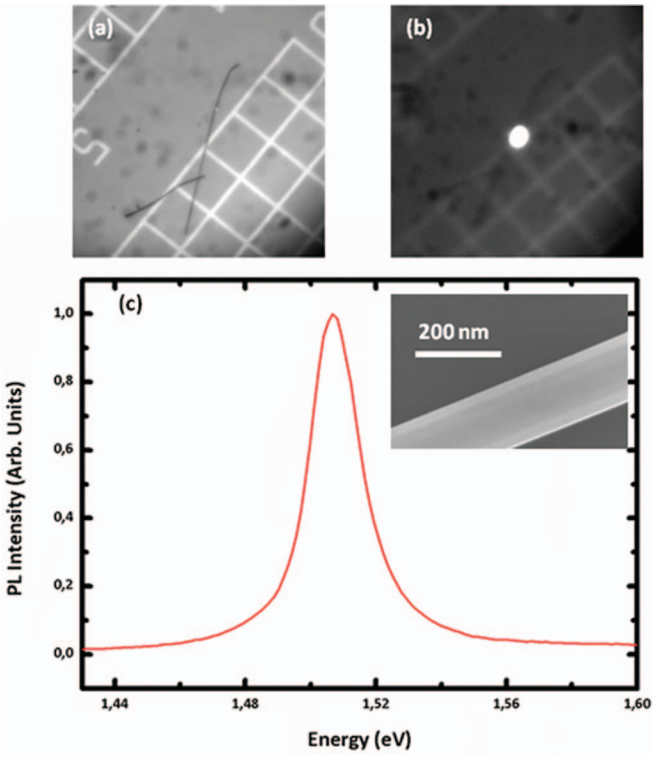

FIG. 2. (a) Optical microscope image, under white light excitation, showing two GaAs NWs deposited on a silicon substrate with a square grid of 15 μm. The longer NW one has a length of about 60 μm. (b) Same image as (a) but under focused laser excitation of the longer NW at 10 K and with filters at the detection selecting only the luminescence emission. This image reveals a bright spot due to local microluminescence of the NW. (c) Microluminescence spectrum of the emission shown in (b). Shown in the inset is a MEB image of the longer NW.

For GaAs NWs grown in this work by VLS-HVPE, the peak position, at 1.507 eV, occurs at an energy about 12 meV below the bulk bandgap. This difference could be due to heating of the sample by the tightly-focused laser excitation, to a temperature of the order of 75 K. The linewidth measured here is smaller (18 meV) with respect to 50 meV for GaAs NWs grown by VLS-MOVPE.[34] It is worth noting that the optical properties are comparable to those of NWs grown by catalyst-free MBE process[35,36] with no WZ emission contribution between 1.43 eV and 1.48 eV. Note finally that, unlike images of the luminescence emission obtained on bulk GaAs which are circular,[32] the image (Fig. 2(b)) shows a spot which is slightly elliptic with the major axis aligned along the length of the NW. While it is tempting to ascribe this to photo-electron transport along the NW, the spatial resolution and mechanical stability of the microscope are not yet sufficient to analyze the form of the microluminescence spot quantitatively. It is only possible to tentatively conclude that the photoelectron diffusion length is larger than approximately 2 μm.

III. PROOF THE PRESENT GaAs NANOWIRES ARE POLYTYPISM FREE

Morphological and structural properties of the GaAs NWs were investigated by TEM and high resolution transmission electron microscopy (HRTEM). GaAs samples were put in ethanol and sonicated for 10 min to separate the NWs from the substrates. A few drops of the resulting solution were then put on a copper grid covered by a carbon film filled with holes. Figure 3(a) shows the TEM image of a rod-like NW 37 μm long and 50 nm in diameter. The remarkable feature of NWs grown by HVPE is their constant diameter over outstanding lengths. The NWs lie on the carbon-coated grid and their growth direction, found to be ⟨111⟩, is in plane. Consequently only the zone axis perpendicular to the growth direction can be observed (Fig. 3(b)). NWs were all indexed in the cubic sphalerite (zinc blende) crystallographic structure, i.e., the normal bulk structure for GaAs (see FFT in Fig. 3(b)) without any polytypism ZB-WZ observed through the entire length of NWs. As for NWs with larger diameter (100 nm),[21] these 50 nm-diameter NWs were found to be hexagonal with {121} facets.

The pure ZB structure was confirmed by Raman spectra recorded on a single GaAs NW in different regions of the NW (Fig. 4(a)). Raman scattering measurements were performed at room temperature with a micro-Raman using the 514.5 nm line of an Ar+ laser as excitation with a spot diameter of about a few μm. Two main scattering peaks are observed, which are located around 263.7 cm^{-1} and 286.1 cm^{-1}, corresponding to the LO and TO phonon modes of ZB GaAs.[36,37] A further signal at about 300 cm^{-1} is observed, which can be ascribed to the silicon substrate.

The synthesis of such long NWs (100 μm) in such a short duration (30 min) could be explained by the physics of

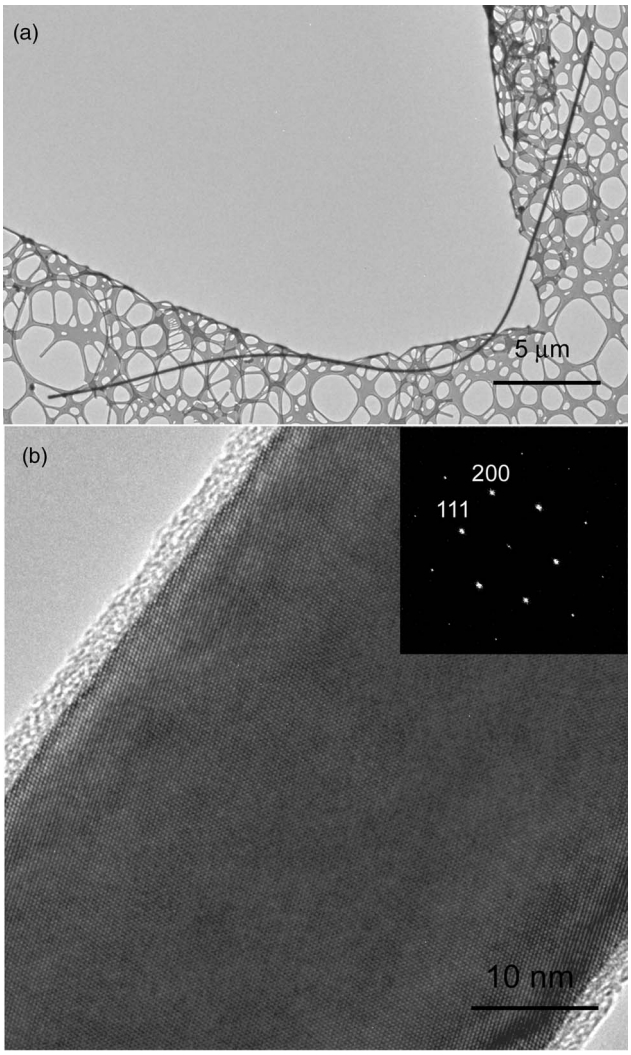

FIG. 3. (a) Image of a single GaAs nanowire 50 μm long and 50 nm in diameter grown at 715 °C. (b) HREM image of the same nanowire taken along the [01-1] zone axis of the zinc blende structure (see FFT). The growth direction is ⟨111⟩. Except near the neck, no stacking faults were observed.

HVPE growth. Given the growth temperature (715 °C), there is no doubt that the Au-Ga droplets should be liquid with an original high percentage of Ga after annealing of the Au-covered GaAs substrates before growth.[38] When switching to the growth fluxes, As and GaCl species adsorb onto the catalyst droplet surfaces and diffuse into the liquid droplets. Fast solidification (up to 170 μm/h) takes place because of the typical HVPE high influxes of As and Ga (70 Pa and 310 Pa respectively), assisted by the high decomposition frequency of GaCl after adsorption. This predominant feeding through the liquid-solid interface with no mass and kinetic hindrance favors axial rather than radial growth. As a matter of fact, the high growth temperature and the constant diameter of NWs grown by VLS-HVPE over length greater than 10 μm excludes any surface diffusion of precursors from the surface of the substrate along the NWs sidewalls, the latter being proven to yield tapering of NWs exhibiting a larger base.[39]

Moreover, GaAs NW VLS-HVPE growth takes place in a H_2/HCl ambient pressure. Radial growth is suppressed when using additional HCl flow as observed for the VLS-MOVPE growth of GaP and InP NWs, for which *in situ* etching is supposed to induce significant axial and radial growth anisotropy.[40,41] In the case of HVPE, additional HCl is a common experimental parameter that is used to vary the vapor supersaturation and consequently, the growth rate of oriented crystal face.[26] As a matter of fact, we cannot exclude that the {121} lateral facets of GaAs NWs exposed to the vapor phase for direct condensation may not grow for the HCl additional partial pressure that was used for the growth of the NWs.

The peculiar feature of NWs grown by HVPE presented here is that they have absolutely no stacking faults or twins over lengths of several tens of microns, which is better than results reported elsewhere. As discussed by Glas *et al.*,[14] the ZB structure is certainly favored because of the nucleation mechanism which takes place at the center of the catalyst droplet. This is consistent with the hypothesis of preferential supply of matter through the catalyst droplet in HVPE.

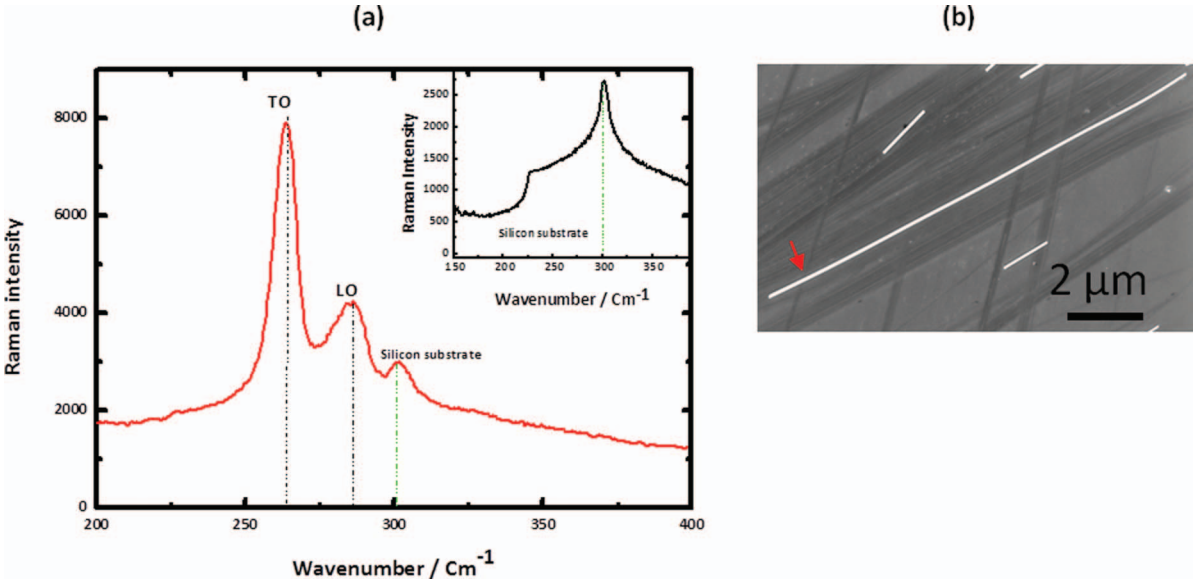

FIG. 4. (a) Raman spectra of a single GaAs nanowire grown at 715 °C. (b) SEM image of the GaAs nanowire deposited on a silicon substrate, indicating the points where the Raman spectra were recorded.

The resulting high Ga concentration in the droplet decreases the surface energy of the latter, which inhibits nucleation at the triple phase line,[14] thus preventing the formation of the WZ structure. Maintaining a stable liquid supersaturation in the droplet avoids the formation of stacking faults and twins, leading to polytypism-free NWs.[14]

IV. DENSITY FUNCTIONAL THEORY SUPPORTING FAST GALLIUM DIFFUSION IN THE CATALYST DROPLET

In order to test the assumption of direct and fast feeding of Ga atoms towards the liquid-NW solid interface in the droplet, an *ab initio* method has been developed to model the diffusion of the Ga atoms in the droplet. We have considered in this first approach the initial stage of growth with an Au-Ga catalyst droplet. The ABINIT software[42] which implements the density functional theory is used, replacing the core-electrons by a pseudo-potential.[43] A periodic slab was defined, first with a double layer of gold atoms on the GaAs (001) face and repeated on the perpendicular axis. This allows the Brillouin zone to be defined for the system. Numerical calculations of energetics are carried out in k-space (using the PBE functional[44]). While the DFT work described so far was applied to static structures, movement of atoms is essential in the observed phenomena. This requires a DFT based *ab initio* dynamics approach.

The Car-Parrinello dynamics method is used because it provides *ab initio* dynamics at drastically reduced computational cost. It combines Ehrenfest and Born-Oppenheimer dynamics. In particular, the time scale and time step used for integrating the equations of motion are governed by those characteristic of the electrons, since their intrinsic motion is far more rapid than that of nuclei. The electron density provides a term in the Lagrangian. This is evaluated by solving the Kohn-Sham equations, over a plane-wave basis, for periodic systems. A fictitious mass (μ) is ascribed to the density and the motion deduced from the following Lagrangian with the constraint of normation:[45]

$$\iota_{cp} = \frac{1}{2}\mu \sum_i \int |\dot{\psi}_\iota(\vec{r})|^2 d\vec{r} + \frac{1}{2}\sum_\iota M_\iota \dot{\vec{R}}_\iota^2 + \sum_{i,j} \Lambda_{ij}\left(\int \psi_i^*(\vec{r})\psi_j(\vec{r})d\vec{r} - \delta_{ij}\right) - \varepsilon_e[\{\psi_i\}, \{\vec{R}_\iota\}].$$

Diffusion of gallium atoms from the exterior gold drop surface to the gold-GaAs interface is expected to be rapid, because the metallic radii of gold and Ga are very similar (136 and 135 pm) and, at the growth temperature, the gold is liquid. This diffusion is simulated by Car-Parrinello dynamics[45] and followed by plotting the co-ordinates of one (or a few) Ga atoms perpendicular to the interface. This shows them moving through the gold and rapidly reaching the interface. The simulation takes a double layer of gold with gallium atoms initially outside it. Various geometries are allowed to relax. Table I chooses ten geometries (plotting h, the perpendicular distance or height above the GaAs surface), including the initial values and compares them to the bound state of Ga, above an octahedral interstice of GaAs. Note that the final position of the Ga atom tends to be at a shorter distance, suggesting higher co-ordination (including by gold atoms). A single Ga atom only moves far enough to displace that in the interstice below, in a fast cascade mechanism. Note the gold liquid relaxes slightly as the Ga atom passes through it, the first layer of atoms being perturbed more than the second. Overall, this is a small effect (initial height 2.77, 3.42 final for layer 1 and initial 7.67, 7.82 final for layer 2 in Table I). Figure 5 gives the atom positions in a hemi-spherical drop of $Au_{16}Ga_4$ positioned with the GaAs surface at z = h = 0. The Gallium atom followed during diffusion is initially outside the drop and finally at a binding distance from the surface, having rapidly been transferred through it (compare positions of Table I with gold drop structure and coordinates in Fig. 5).

TABLE I. Position of diffusing Ga atoms (column 2) in a bilayer of gold (Au_1 and Au_2), height in bohr (column 1).

Height in bohr	Ga	Au_1	Au_2
Init	9.67	2.77	7.67
1	5	2.77	7.67
2	3.71	3.02	7.91
3	3.62	3.12	8.02
4	2.31	3.14	8.06
5	2.12	3.16	8.07
6	2.05	3.17	8.06
7	2.03	3.18	8.06
8	2.01	3.23	8.01
9	1.99	3.42	7.82

The diffusion coefficient of Ga atoms was estimated as 3×10^{-9} m^2/s. This value is in good agreement with those from a thermodynamic model proposed by Lui *et al.*,[46] who gave an *ad hoc* expression for varying composition and temperature in liquid metal.

Analytical one dimension solution of Fick's law diffusion, with the above bulk diffusion constant, shows that on the timescale of growth, nearly all of a large number of gallium atoms diffuse through two layers of gold to the interface with GaAs: for 4 and 30 min, the fraction remaining is only 5×10^{-5} and 10^{-5}, respectively. This corresponds to experimental observation. The post-growth EDS analysis showed a Ga content below 1% in the tip of grown NWs.[21] This supports observations of fast growth with piling of GaAs at the interface with the gold.

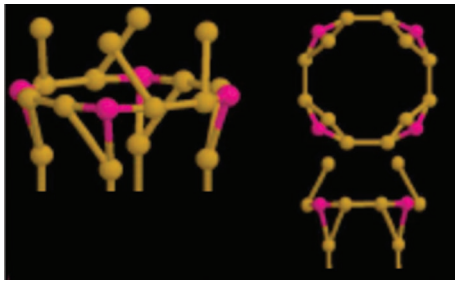

FIG. 5. Geometry optimization of the $Au_{32}Ga_8$ droplet. The golden dots represent Gold atoms and pink dots represent the Gallium atoms. The successive optimizations of the droplet correspond to the Car and Parrinello step 3.

V. CONCLUSION

Catalyst-assisted VLS growth in a HVPE environment lead to the synthesis at high axial growth rate of ultra-long rod-like shape GaAs nanowires with pure zinc blende crystal quality with a 50 nm mean diameter, as shown by HRTEM, FFT and Raman spectroscopy analyses. Photoluminescence measurements highlighted the good quality of single NWs with linewidth of 18 meV. The growth mechanisms were discussed for high growth temperature (715 °C) which yields fast decomposition of the chloride GaCl growth precursors. The diffusion coefficient of Ga atoms was calculated. It is high indeed and consistent with the observed NWs high growth rates and the favored cubic structure after nucleation at the liquid-solid interface at the center of the NWs. Steady experimental conditions in terms of vapor supersaturation and consequent liquid supersaturation induce the growth of remarkable polytypism-free NWs on lengths of several tens of microns in short growth times.

ACKNOWLEDGMENTS

This work was supported by Région Auvergne and the European Union under FEDER grants (CPER 2007-2013). The authors wish to thank Vladimir Dubrovkii for discussions and help.

[1]S. A. Dayeh, C. Soci, X. Y. Bao, and D. Wang, Nano Today **4**, 347 (2009).
[2]M. Heiss, Y. Fontana, A. Gustafsson, G. Wüst, C. Magen, D. D. O'Regan, J. W. Luo, B. Ketterer, S. Conesa-Boj, A. V. Kuhlmann, J. Houel, E. Russo-Averchi, J. R. Morante, M. Cantoni, N. Marzari, J. Arbiol, A. Zunger, R. J. Warburton, and A. i Morral Fontcuberta, Nat. Mater. **12**, 439 (2013).
[3]J. A. Czaban, D. A. Thompson, and R. R. LaPierre, Nano Lett. **9**, 148 (2009).
[4]C. Colombo, P. Krogstrup, J. Nygård, M. L. Brongersma, and A. i Morral Fontcuberta, New J. Phys. **13**, 123026 (2011).
[5]E. Uccelli, J. Arbiol, C. Magen, P. Krogstrup, E. Russo-Averchi, M. Heiss, G. Mugny, F. O. Morier-Genoud, J. Nygård, J. R. Morante, and iMorral A. Fontcuberta, Nano Lett. **11**, 3827 (2011).
[6]G. Patriarche, F. Glas, M. Tchernycheva, C. Sartel, L. Largeau, J. C. Harmand, and G. E. Cirlin, Nano Lett. **8**, 1638 (2008).
[7]A. I. Persson, M. W. Larsson, S. Stenström, B. J. Ohlsson, L. Samuelson, and L. R. Wallenberg, Nat. Mater. **3**, 677 (2004).
[8]K. A. Dick, P. Caroff, J. Bolinsson, M. E. Messing, J. Johansson, K. Deppert, L. R. Wallenberg, and L. Samuelson, Semicond. Sci. Technol. **25**, 024009 (2010).
[9]H. Shtrikman, R. Popovitz-Biro, A. Kretinin, L. Houben, M. Heiblum, M. Bukala, M. Galicka, R. Buczko, and P. Kacman, Nano Lett. **9**, 1506 (2009).
[10]H. J. Joyce, Q. Gao, H. H. Tan, C. Jagadish, Y. Kim, J. Zou, L. M. Smith, H. E. Jackson, J. M. Yarrison-Rice, P. Parkinson, and M. B. Johnston, Prog. Quantum Electron. **35**, 23 (2011).
[11]J. Bao, D. C. Bell, F. Capasso, J. B. Wagner, T. Mårtensson, J. Tragardh, and L. Samuelson, Nano Lett. **8**, 836 (2008).
[12]K. Pemasiri, M. Montazeri, R. Gass, L. M. Smith, H. E. Jackson, J. Yarrison-Rice, S. Paiman, Q. Gao, H. H. Tan, C. Jagadish, X. Zhang, and J. Zou, Nano Lett. **9**, 648 (2009).
[13]R. L. Woo, R. Xiao, Y. Kobayashi, L. Gao, N. Goel, M. K. Hudait, T. E. Mallouk, and R. F. Hicks, Nano Lett. **8**, 4664 (2008).
[14]F. Glas, J. C. Harmand, and G. Patriarche, Phys. Rev. Lett. **99**, 146101 (2007).
[15]H. J. Joyce, Q. Gao, H. H. Tan, C. Jagadish, Y. Kim, M. A. Fickenscher, S. Perera, T. B. Hoang, L. M. Smith, H. E. Jackson, J. M. Yarrison-Rice, X. Zhang, and J. Zou, Nano Lett. **9**, 695 (2009).
[16]P. Krogstrup, R. Popovitz-Biro, E. Johnson, M. H. Madsen, J. Nygård, and H. Shtrikman, Nano Lett. **10**, 4475 (2010).
[17]H. Shtrikman, R. Popovitz-Biro, A. Kretinin, and M. Heiblum, Nano Lett. **9**, 215 (2009).
[18]H. J. Joyce, Q. Gao, H. H. Tan, C. Jagadish, Y. Kim, X. Zhang, Y. Guo, and J. Zou, Nano Lett. **7**, 921 (2007).
[19]H. J. Joyce, Q. Gao, H. H. Tan, C. Jagadish, Y. Kim, M. A. Fickenscher, S. Perera, T. B. Hoang, L. M. Smith, H. E. Jackson, J. M. Yarrison-Rice, X. Zhang, and J. Zou, Adv. Funct. Mater. **18**, 3794 (2008).
[20]X. Ren, H. Huang, V. G. Dubrovskii, N. V. Sibirev, M. V. Nazarenko, A. D. Bolshakov, X. Ye, Q. Wang, Y. Huang, X. Zhang, J. Guo, and X. Liu, Semicond. Sci. Technol. **26**, 014034 (2011).
[21]M. R. Ramdani, E. Gil, Ch. Leroux, Y. André, A. Trassoudaine, D. Castelluci, L. Bideux, G. Monier, C. Robert-Goumet, and R. Kupka, Nano Lett. **10**, 1836 (2010).
[22]K. Lekhal, G. Avit, Y. André, A. Trassoudaine, E. Gil, C. Varenne, C. Bougerol, G. Monier, and D. Castelluci, Nanotechnology **23**, 405601 (2012).
[23]F. Lassalle, A. Porte, J. L. Laporte, C. Pariset, and R. Cadoret, Mater. Res. Bull. **23**, 1285 (1988).
[24]A. Pimpinelli, R. Cadoret, E. Gil-Lafon, J. Napierala, and A. Trassoudaine, J. Cryst. Growth **258**, 1 (2003).
[25]E. Gil-Lafon, J. Napierala, A. Pimpinelli, R. Cadoret, A. Trassoudaine, and D. Castelluci, J. Cryst. Growth **258**, 14 (2003).
[26]E. Gil-Lafon, J. Napierala, D. Castelluci, A. Pimpinelli, R. Cadoret, and B. Gerard, J. Cryst. Growth **222**, 482 (2001).
[27]L. Bideux, G. Monier, V. Matolin, C. Robert-Goumet, and B. Gruzza, Appl. Surf. Sci. **254**, 4150 (2008).
[28]G. Monier, L. Bideux, C. Robert-Goumet, B. Gruzza, M. Petit, J. L. Lábáre, and M. Menyhárd, Surf. Sci. **606**, 1093 (2012).
[29]C. Chatillon and D. Chatain, J. Cryst. Growth **151**, 91 (1995).
[30]M. C. Plante, J. Garrett, S. C. Ghosh, P. Kruse, H. Schriemer, T. Hall, and R. R. LaPierre, Appl. Surf. Sci. **253**, 2348 (2006).
[31]J. S. Blakemore, J. Appl. Phys. **53**, R123 (1982).
[32]I. Favorskiy, D. Vu, E. Peytavit, S. Arscott, D. Paget, and A. C. H. Rowe, Rev. Sci. Instrum. **81**, 103902 (2010).
[33]B. V. Novikov, S. Y. Serov, N. G. Filosofov, I. V. Shtrom, V. G. Talalaev, O. F. Vyvenko, E. V. Ubyivovk, Y. B. Samsonenko, A. D. Bouravleuv, I. P. Soshnikov, N. V. Sibirev, G. E. Cirlin, and V. G. Dubrovskii, Phys. Status Solidi RRL **4**(7), 175 (2010).
[34]V. Dhaka, T. Haggren, H. Jussila, H. Jiang, E. Kauppinen, T. Huhtio, M. Sopanen, and H. Lipsanen, Nano Lett. **12**, 1912 (2012).
[35]S. Ambrosini, M. Fanetti, V. Grillo, A. Franciosi, and S. Rubini, J. Appl. Phys. **109**, 094306 (2011).
[36]D. Spirkoska, J. Arbiol, A. Gustafsson, S. Conesa-Boj, F. Glas, I. Zardo, M. Heigoldt, M. H. Gass, A. L. Bleloch, S. Estrade, M. Kaniber, J. Rossler, F. Peiro, J. R. Morante, G. Abstreiter, L. Samuelson, and A. i Morral Fontcuberta, Phys. Rev. B **80**, 245325 (2009).
[37]N. Begum, M. Piccin, F. Jabeen, G. Bais, S. Rubini, F. Martelli, and A. S. Bhatti, J. Appl. Phys. **104**, 104311 (2008).
[38]T. B. Massalski, *Binary Alloy Phase Diagrams* (American Society for Metals, 1990), Vol. 1.
[39]M. C. Plante and R. R. Lapierre, J. Cryst. Growth **286**, 394 (2006).
[40]S. Assali, I. Zardo, S. Plissard, D. Kriegner, M. A. Verheijen, G. Bauer, A. Meijerink, A. Belabbes, F. Bechstedt, J. E. M. Haverkort, and E. P. A. M. Bakkers, Nano Lett. **13**, 1559 (2013).
[41]M. T. Borgström, J. Wallentin, J. Trägardh, P. Ramwall, M. Ek, L. Reine Wallenberg, L. Samuelson, and K. Deppert, Nano Res. **3**, 264 (2010).
[42]X. Gonze, J. M. Beuken, R. Caracas, F. Detraux, M. Fuchs, G. M. Rignanese, L. Sindic, M. Verstraete, G. Zerah, F. Jollet, M. Torrent, A. Roy, M. Mikami, P. Ghosez, J. Y. Raty, and D. C. Allan, Comput. Mater. Sci. **25**, 478 (2002).
[43]M. Fuchs and M. Scheffler, Comput. Phys. Commun. **119**, 67 (1999).
[44]J. P. Perdew, K. Burke, and M. Ernzerhof, Phys. Rev. Lett. **77**, 3865 (1996).
[45]R. Car and M. Parrinello, Phys. Rev. Lett. **55**, 2471 (1985).
[46]Y. Liu, Z. Long, H. Wang, Y. Du, and B. Huang, Scr. Mater. **55**, 367 (2006).